

Oscillatory tunnel magnetoresistance in double barrier magnetic tunnel junctions

Zhong-Ming Zeng, Xiu-Feng Han,* and Wen-Shan Zhan

State Key Laboratory of Magnetism and Laboratory of Microfabrication, Beijing National Laboratory for Condensed Matter Physics, Institute of Physics, Chinese Academy of Science, Beijing 100080, China

Yong Wang and Ze Zhang

Laboratory of Advanced Materials and Electron Microscopy, Institute of Physics, Chinese Academy of Science, Beijing 100080, China

Shufeng Zhang

Department of Physics and Astronomy, University of Missouri-Columbia, Columbia, Missouri 65211, USA

(Received 22 June 2005; published 15 August 2005)

We report an unconventional oscillatory tunnel magnetoresistance as a function of the applied bias in double barrier magnetic tunnel junctions that were made of two Al_2O_3 barriers sandwiched by three ferromagnetic layers. When the center ferromagnetic layer is aligned antiparallel to the top and bottom magnetic layers, a distinct magnetoresistance oscillation appears with respect to the increase of the bias voltage at 4.2 K and at room temperature. The period of the oscillation is about 1.6 mV.

DOI: [10.1103/PhysRevB.72.054419](https://doi.org/10.1103/PhysRevB.72.054419)

PACS number(s): 75.47.-m, 72.25.Ba, 75.70.Cn, 85.75.Mm

I. INTRODUCTION

Since the high tunnel magnetoresistance (TMR) at room temperature (RT) was discovered a decade ago,^{1,2} the quality of tunnel junctions continues to improve. Recently, very large TMR values have been achieved in several systems due to much improved interface morphology between the barrier and electrodes by using various materials combinations.³⁻⁵ These advances will not only accelerate the development of magnetic random access memory (MRAM) and magnetic reading heads, but also open a door to fabricate a more complicated system, e.g., double barrier magnetic tunnel junctions (DBMTJs), to further study physics of spin-dependent tunneling. In a DBMTJ, the center metal layer, magnetic or nonmagnetic, is confined by two high potential barriers, and thus one might expect (1) formation of the quantum well states and (2) resonant tunneling if the bias voltage matches with the energy of the quantum well states. To observe these effects, the DBMTJ must be of an extremely high quality. Otherwise the above effects will be washed away due to interface roughness and impurity scattering. In semiconductor heterostructure, the resonant tunneling has become one of the standard tools in probing electronic structure of the materials. However, for the DBMTJ, experiments had failed to observe coherent tunneling up till now although considerable progress on both theoretical and experimental studies had been performed.⁶⁻¹² Our recent success¹³ on the fabrication of high quality MTJs prompts us to grow smoother interfaces of the DBMTJs so that we intend to address these interesting phenomena with our improved MTJs.

In this paper, we report an unusual magnetotransport phenomenon observed in the DBMTJ. We have found that the conductance (resistance R_{AP}) for the antiparallel aligned state, i.e., the magnetization of the center (free) magnetic layer is antiparallel to the magnetization of the two outer (pinned) magnetic layers, shows distinct oscillations with respect to the applied bias voltage. However, for the parallel

aligned state, no conductance (resistance R_p) oscillation is observed. This feature can not be simply attributed to the resonant tunneling in the antiparallel state. In fact, we will show that the resonant model fails to capture the main characteristics of our data. We have proposed a model involving spin accumulation induced magnon assisted tunneling. However, we point out that the quantitative explanation requires a novel theory beyond a simple elastic resonant tunneling.

II. SAMPLE PREPARATION AND CHARACTERIZATION

The DBMTJs with a complete layering sequence

$$\begin{aligned} & \text{Si/SiO}_2\text{-Sub/Ta(5)/Cu(30)/Ta(5)/Ni}_{79}\text{Fe}_{21}(10)/\text{Ir}_{22}\text{Mn}_{78}(12)/ \\ & \text{Co}_{75}\text{Fe}_{25}(4)/\text{Ru}(0.9)/\text{Co}_{75}\text{Fe}_{25}(4)/\text{Al}(1)\text{-oxide}/ \\ & \text{Co}_{75}\text{Fe}_{25}(1)/\text{Ni}_{79}\text{Fe}_{21}(2)/\text{Co}_{75}\text{Fe}_{25}(1)/\text{Al}(1)\text{-oxide}/ \\ & \text{Co}_{75}\text{Fe}_{25}(4)/\text{Ru}(0.9)/\text{Co}_{75}\text{Fe}_{25}(4)/\text{Ir}_{22}\text{Mn}_{78}(12)/ \\ & \text{Ni}_{79}\text{Fe}_{21}(10)/\text{Cu}(30)/\text{Ta}(5) \end{aligned}$$

were fabricated by using an ULVAC TMR R&D Magnetron Sputtering (MPS-4000-HC7), where the numbers in parentheses have a unit of nanometer. A brief explanation of the above structure is as follows. The center (free) magnetic layer $\text{Co}_{75}\text{Fe}_{25}(1)/\text{Ni}_{79}\text{Fe}_{21}(2)/\text{Co}_{75}\text{Fe}_{25}(1)$ was sandwiched by two Al(1)-oxide barriers. The two outer (pinned) ferromagnetic layers, $\text{Co}_{75}\text{Fe}_{25}(4)$, were coupled through Ru spacers and two $\text{Ir}_{22}\text{Mn}_{78}(12)$ were antiferromagnetic layers which supply exchange bias fields to the outer magnetic layers. The multilayers were deposited at a base pressure below 5×10^{-7} Pa without breaking vacuum. An in-plane magnetic field of 100 Oe was applied during the growth to define the uniaxial magnetic anisotropy of the magnetic layers. The sputtering pressure with Ar gas was 0.07 Pa. The Al_2O_3 barrier was formed by inductively coupled plasma (ICP) oxidizing 1 nm Al-layer with an oxidation time of 55 s in a mixture of oxygen and argon at a pressure of 1.0 Pa in a separate

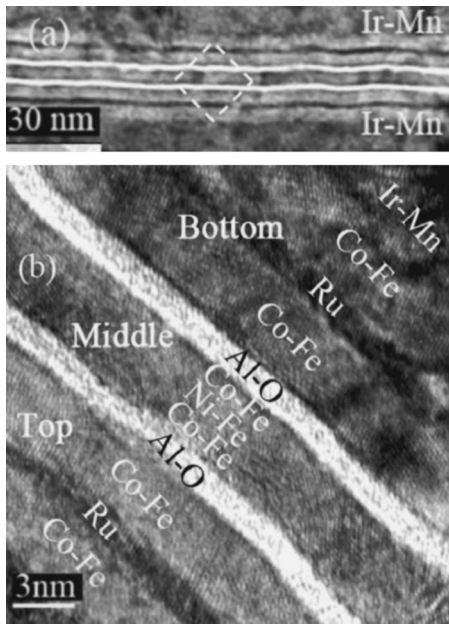
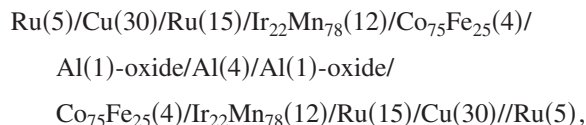


FIG. 1. A cross-sectional HRTEM image of a typical DBMTJ and (b) is the magnified image of the square part as shown that in (a).

plasma oxidation chamber. The ellipse shaped DBMTJs with the junction area of $\pi \times 3 \times 6 \mu\text{m}^2$ were formed by photolithography and Ar-ion etching techniques.¹² All the micro-fabrication processes were done in a clean room. The quality of the layered structure was examined by cross-sectional high resolution transmission electron microscopy (HRTEM) image combined with the magnetoelectric transport analysis. The magnetic properties were characterized by the Physical Properties Measurement System (Model PPMS-14T) made in American Quantum Design and also the transport properties were measured via a four-probe method.

Figure 1 shows a cross-sectional HRTEM image of a typical DBMTJ. Both parallel Al-O tunnel barriers display an amorphous structure and no pinhole defects were spotted across the sample. The thickness of each barrier is estimated to be between 1.1 and 1.3 nm; this is near to the generic Al deposition thickness of 1.0 nm. The interface roughness is correlated for both tunnel barriers. The bottom barrier seems smoother than the top barrier to some extent. By comparing the HRTEM images for the as-deposited and annealed samples (see below for the annealing conditions), we find that annealing promotes the smoothing of the roughness and the properly annealed samples have larger TMR values.

In order to exactly determine the switching field and the component of magnetization for each magnetic layer, besides of the same DBMTJ film, other MTJ films with the similar layer structures of



or

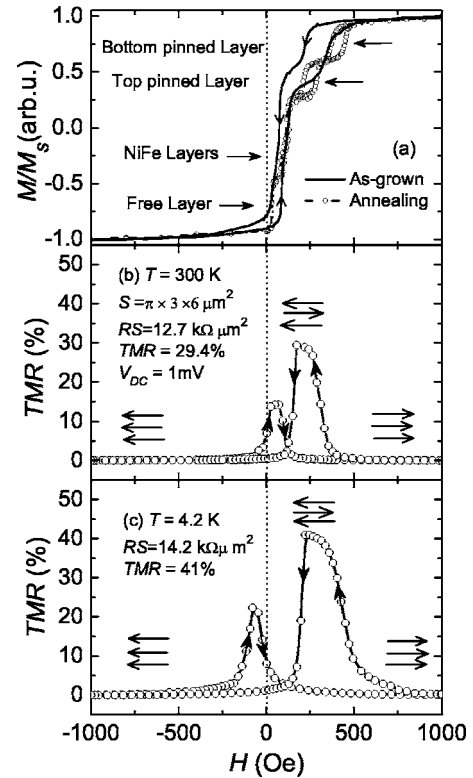
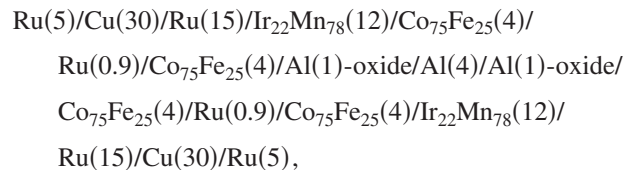
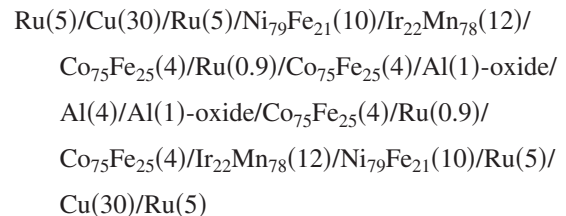


FIG. 2. Normalized magnetization vs magnetic field curves of the same DBMTJ film at as-deposited and after annealing states (a), TMR versus the magnetic field curves measured at RT (b) and at 4.2K (c) for the patterned DBMTJ.



and



were also deposited on the Si/SiO₂ wafer using the same experimental conditions. Then the magnetization versus the magnetic field curves of the such MTJ films were measured separately using a vibrating sample method (VSM, DMS MODEL 4 HF, made in American ADE Company).

III. EXPERIMENTAL RESULTS

Figure 2(a) shows the normalized magnetization versus the magnetic field curves of the same DBMTJ film measured separately using the VSM before patterning in order to confirm the existence of the AP and P states. It can

be seen that the magnetization of the free layer $\text{Co}_{75}\text{Fe}_{25}(1)/\text{Ni}_{79}\text{Fe}_{21}(2)/\text{Co}_{75}\text{Fe}_{25}(1)$, both the top and bottom buffer layers $\text{Ni}_{79}\text{Fe}_{21}(10)$, and both the top and bottom artificially pinned layers $\text{Co}_{75}\text{Fe}_{25}(4)/\text{Ru}(0.9)/\text{Co}_{75}\text{Fe}_{25}(4)$ rotated one by one with increasing external magnetic field from 0 to +1000 Oe or from +1000 to 0 Oe for two forth and back magnetization curves. The magnetization rotation for each magnetic layer was observed distinctly by each clear step. The reversal of the free layer was offset by around 40 Oe due to the interlayer coupling and the orange-peel coupling upon the interface roughness between the free and pinned layers. It can be confirmed that for our sample at as-deposited and after annealing states the antiparallel configuration between the free layer of $\text{Co}_{75}\text{Fe}_{25}(1)/\text{Ni}_{79}\text{Fe}_{21}(2)/\text{Co}_{75}\text{Fe}_{25}(1)$ and both the top and bottom pinned layers of $\text{Co}_{75}\text{Fe}_{25}(4)/\text{Ru}(0.9)/\text{Co}_{75}\text{Fe}_{25}(4)$ appeared in the forth magnetization curve at around 200 Oe and in back magnetization curve at around 100 Oe. Here, it is noted that although we have designed antiferromagnetic coupling for each one of two artificial pinned layers of $\text{Co}_{75}\text{Fe}_{25}(4)/\text{Ru}(0.9)/\text{Co}_{75}\text{Fe}_{25}(4)$, we observed experimentally the ferromagnetic coupling across the Ru layers. However, this coupling does not affect the parallel and antiparallel configurations between the free layer and two top and bottom pinned layers as appeared in the forth and back magnetization shown in Fig. 2(a). It is also noted that the switching field for the two top and bottom artificial pinned layers at the as-deposited state had almost same value, whereas different switching fields appeared upon annealing as seen from two steps in the loop for the annealed sample. The annealing may cause a change in the grain size, textures, and interface roughness.¹⁴ The patterning can also change the switching characteristics. Thus it is not be surprised that the resistance peaks shown in Figs. 2(b) and 2(c) are not exactly the AF aligned state measured in the hysteresis loop of un-patterned films.

The DBMTJ samples reported below were annealed for an hour at 533 K. During the annealing, a magnetic field of 1 kOe was applied in the easy axis direction. Since the annealing temperature is close to the Blocking temperature of Ir-Mn,¹⁵ the applied field sets the direction of the exchange bias. We found the exchange bias H_E is about 170 Oe at 4.2 K and 100 Oe at room temperature for both top and bottom electrodes. Figures 2(b) and 2(c) are typical results on the TMR versus the magnetic field measured at RT and 4.2 K for the patterned DBMTJ samples after annealing. At a large negative magnetic field, the magnetization of three magnetic layers is aligned along the direction of the magnetic field. In this case, the tunnel resistance is minimum and we denote it as R_P . When the magnetic field increases to a certain positive value, the middle free magnetic layer begins to reverse its direction while both top and bottom artificially pinned (outer) layers remained their original direction, i.e., the magnetization of the middle free layer is now oriented antiparallel to the magnetization of the two outer layers. In this case, the resistance of the DBMTJ is maximum and we define it as R_{AP} . Since the exchange bias field for the top and the bottom artificial pinned layers is approximately same, the further increase of the magnetic field reverses the magneti-

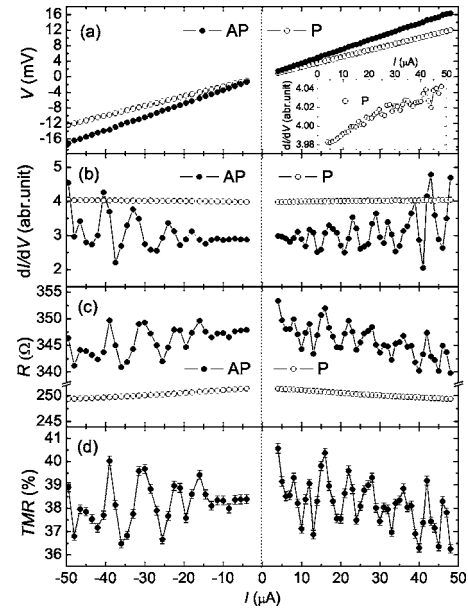


FIG. 3. Bias voltage (a), differential conductance dI/dV (b), tunnel resistance $R=V/I$ (c) and TMR ratio (d) vs bias current curves at 4.2 K for the patterned DBMTJ. The TMR measuring errors marked in the Fig. 3(d) were determined from the noise amplitude of dI/dV in the P configuration as shown in the inset of Fig. 3(a) located at the right corner.

zation of the two outer layers and the resistance is back to minimum where all three magnetic layers are aligned parallel. If we define the ratio of the tunnel magnetoresistance $R=(R_{AP}-R_P)/R_P$, we find the TMR ratio is about 41% at 4.2 K and 29.4% at RT. If we re-tracked the resistance from the large positive field to the large negative field in Figs. 2(b) and 2(c), we noticed that the resistance peak was much smaller. It was indicating that the perfect antiparallel alignment was not achieved in the reversed magnetic field cycle due to the inconsistent domain switching for the free layer and both the top and bottom artificially pinned layers in the patterned DBMTJs.

Figure 3 shows the bias voltage, differential conductance dI/dV , the tunnel resistance $R=V/I$ and the TMR ratio versus bias current curves at 4.2 K when both the positive and negative bias current were applied from 4 to 50 μA . The polarity of the current is defined as positive when the current flows from the top to the bottom layers of the DBMTJ. To establish I - V characteristics for the P and AP configurations separately, we measured a hysteresis loop as in Fig. 2(c) for each bias current (voltage) and determined the maximum and minimum resistances for each loop at a fixed current density. Therefore, there were more than 150 magneto-resistance versus magnetic field curves which were continuously measured by PPMS in order to deduced the data shown in Figs. 3(a), 3(c), and 3(d). The salient feature shown in the Figs. 3(c) and 3(d) is that R_{AP} and TMR show a strong oscillation with respect to the bias current in the AP configuration. To further confirm the magnetoresistance oscillation phenomenon, the conductance dI/dV versus I or V curves were deduced by differentiating the I - V curves which also showed the oscillations clearly. The period of the oscillation is about 5 μA at

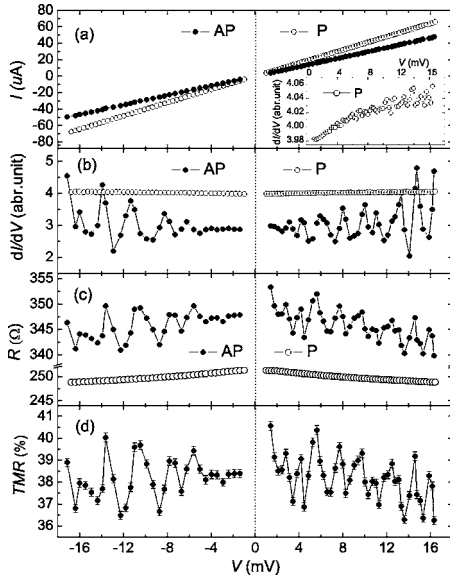


FIG. 4. Bias current (a), differential conductance dI/dV (b), tunnel resistance $R=V/I$ (c) and TMR ratio (d) vs bias voltage curves at 4.2 K for the same patterned DBMTJ. The TMR measuring errors marked in the Fig. 4(d) were determined from the noise amplitude of dI/dV in the P configuration as shown in the inset of Fig. 4(a) located at the right corner.

low temperature. On the other hand, there is no visible oscillation in the P configuration at all. Thus, the oscillation of the TMR ratio, Fig. 3(d), was solely from the oscillation of the resistance in AP states.

Also, when we reverse the polarity of the current, the similar features are seen, although the amplitude and the phase of the oscillation is slightly different from that for the positively biased current, possibly due to asymmetric microstructure of the two barriers. It has been known that the I - V is typically asymmetric for MTJs.

Figure 4 shows the similar behavior for the bias voltage dependence of the differential conductance dI/dV , tunnel resistance R and TMR ratio at 4.2 K for the same patterned DBMTJ because the bias current versus voltage and vice versa have a linear relation in smaller measurement range. The period of the oscillation is about 1.6 mV at low temperature.

The above oscillatory behavior for the AP configuration remains evident at RT, but the amplitude of the oscillation is smaller (data not shown).

IV. DISCUSSIONS

These data call for a new interpretation of the spin-dependent tunneling in the DBMTJ. Before we present our argument on why the observed data are novel, we point out that the above oscillatory magnetoresistance can not be caused by the variation of the domain structure of the magnetic layers. We have noticed that the peak resistance shown in Fig. 2 may not represent the perfect antiferromagnetic state, i.e., it is possible that the magnetization of the middle layer is not completely antiparallel to the magnetization of

the electrodes and the middle layer may not be in a single domain state. However, the question here is that how the domain pattern possibly changes with respect to the applied current in a *periodic manner* shown in the resistance measurement? If we estimate the magnetic field generated by a 5 μ A current, we find the maximum value is only about a fraction of Oe. Such a small field would not affect the domain structure of the DBMTJ in any significant way. Furthermore, there is no mechanisms for the current-induced field to generate a *periodic change* of the magnetization patterns. Thus, the observed effect must be associated with a spin-dependent tunneling mechanism in the DBMTJ.

At this point, we want to compare our results with previous oscillatory tunnel magnetoresistance in other related systems. Nakajima *et al.* investigated a structure where they used $\text{Co}_{80}\text{Pt}_{20}$ particles in place of our middle magnetic layer.¹⁶ In this case, the electron from the left electrode tunnels into the $\text{Co}_{80}\text{Pt}_{20}$ particles and subsequently tunnels to the right electrode. Due to finite size of $\text{Co}_{80}\text{Pt}_{20}$ particles, the tunneling is prohibited if the energy of the tunnel electron is smaller than the charging energy of the particle; this phenomenon is known as the Coulomb blockade. Indeed, they observed a threshold voltage as well as conductance oscillations when the voltage increased from one integer multiple of the Coulomb blockade energy to another. The effect was well explained by the discrete charging effect.^{17,18} However, this explanation does not apply to our case: (1) The charge effect would be equally applicable to P and AP configurations, and yet we observed the oscillation in the AP but not P states, and (2) our middle layer is a continuous layer as shown in our cross-section TEM and thus the charging energy would negligibly small (below 1 μ eV for our size of the middle layer).

An appealing mechanism is the resonant tunneling. Yuasa *et al.* had studied a careful MBE prepared structure consisted of a $\text{Co}/\text{Al}_2\text{O}_3/\text{Cu}/\text{Co}$ stack where the quantum well state of the Cu layer is responsible for their observed resonant tunneling.¹⁹ The tunnel magnetoresistance is an oscillatory function of the Cu layer thickness, indicating the density of states is a periodic function of the thickness of the Cu layer. The TMR also varies with the applied bias, but the variation occurs at much larger voltage scales of the order of a fraction of a volt. In our case, the period of oscillations is only 1.6 mV and we have not tested oscillations for a different thickness of the middle layer. Furthermore, the oscillation in their experiments appeared in both P and AP configurations because both spin up and down channel participates tunneling. Therefore, our data are clearly beyond the mechanism of the above resonant tunneling: (1) If we assume the formation of the quantum well states in the middle in one of the spin channel, e.g., the minority channel, the majority electrons in the electrodes would establish a resonant tunneling in the AP configuration while the minority electrons would also participate a resonant tunneling in the P configuration. The fact that we did not observe any oscillatory feature in the P state rules out the existence of these resonant states. (2) The observed period of the oscillation, 1.6 mV, is too small to account for the energy level spacing of the quantum well state. For the middle layer thickness of 40 \AA , the energy level spacing from the simple estimation of “the particle-in-the-box” is at

least an order of magnitude larger. (3) To obtain the resonant transmission across the double layers, the tunnel time should be smaller than the electron relaxation time in the middle layer. This resonant condition is unlikely met in our case.

We propose that the effect may involve additional inelastic scattering mechanisms, more specifically, spin wave emissions in the middle ferromagnetic layer. In a single barrier MTJ, the spin accumulation at the two sides of the electrodes contributes very little to the resistance because the barrier resistance is much larger than the spin accumulation induced resistance.²⁰ In the DBMTJ, the spin accumulation in the middle ferromagnetic layer would not contribute to the tunneling if one views the DBMTJ as two single barrier MTJ in series. However, an assisted tunnel might occur if the spin accumulation can generate magnons or spin waves in the middle layer, because these excitations may assist the electron tunneled from the first barrier to tunnel through the second barrier. The magnon assisted tunneling has already been estimated²¹ in the study of the temperature and voltage dependence of the TMR. Let us now consider that the middle magnetic layer is antiparallel to the electrodes. The spin direction of the nonequilibrium spin accumulation in the middle layer (tunneling from the electrodes) would be antiparallel to the local magnetization of the middle layer. When the spin accumulation which is proportional to the applied voltage bias exceeds a critical value such that the difference of the chemical potentials between spin-up and down channels is larger than the threshold of the spin wave gap, typically about 1 meV, magnons can be generated and the magnon-assisted tunneling will contribute to the tunnel conductance. In the P state, the spin accumulation is parallel to the local moment and thus the spin wave emission is prohib-

ited by the spin angular momentum conservation, i.e., the magnon-assisted tunneling is suppressed. Our proposed mechanism is similar to Berger's proposal on the current-induced spin wave emissions.²² While the above suggestion provides a plausible explanation to our data and there are several calculations, e.g., by Stein *et al.*,¹⁰ on the spin accumulation, a much refined theory is needed in order to quantitatively explain our observed results.

V. CONCLUSIONS

In conclusion, we have successfully microfabricated the DBMTJs with a free magnetic layer sandwiched by two barriers and two exchange biased outer magnetic layers. We have observed a novel resistance oscillation when the magnetization of the free layer is antiparallel to the pinned layers. It seems the observed phenomenon is not originated from simple resonant tunneling, rather it calls for a new insight into the unconventional spin-dependent tunneling mechanism.

ACKNOWLEDGMENTS

The project was supported by the State Key Project of Fundamental Research of Ministry of Science and Technology Grant Nos. 2001CB610601 and 2002CB613500, China. X.F.H. gratefully thanks the partial support of Distinct Young Researcher Foundation (50325104) and Chinese National Natural Science Foundation (10274103, 50271081). S.Z. acknowledges the support from NSF (DMR-0314456) of the U.S.

*Author to whom correspondence should be addressed. Email: xfhan@aphy.iphy.ac.cn

¹T. Miyazaki and N. Tezuka, *J. Magn. Magn. Mater.* **139**, L231 (1995).

²J. S. Moodera, L. R. Kinder, T. M. Wong, and R. Meservey, *Phys. Rev. Lett.* **74**, 3273 (1995).

³S. S. Parkin, C. Kaiser, A. Panchula, P. M. Rice, B. Hughes, M. Samant, and S.-H. Yang, *Nat. Mater.* **3**, 862 (2004).

⁴S. Yuasa, T. Nagahama, A. Fukushima, Y. Suzuki, and K. Ando, *Nat. Mater.* **3**, 868 (2004).

⁵D. D. Djayaprawira, K. Tsunekawa, M. Nagai, H. Maehara, S. Yamagata, and N. Watanabe, S. Yuasa, Y. Suzuki, and K. Ando, *Appl. Phys. Lett.* **86**, 092502 (2005).

⁶X. Zhang, B.-Z. Li, G. Sun, and F.-C. Pu, *Phys. Rev. B* **56**, 5484 (1997).

⁷F. Montaigne, J. Nassar, A. Vaurés, F. Nguyen Van Dau, F. Petroff, A. Schuhl, and A. Fert, *Appl. Phys. Lett.* **73**, 2829 (1997).

⁸L. Sheng, Y. Chen, H. Y. Teng, and C. S. Ting, *Phys. Rev. B* **59**, 480 (1999).

⁹Y. Saito, M. Amano, K. Nakajima, S. Takahashi, M. Sagoi, and K. Inomata, *Jpn. J. Appl. Phys., Part 2* **39**, L1035 (2000).

¹⁰S. Stein, R. Schmitz, and H. Kohlstedt, *Solid State Commun.*

117, 599 (2001).

¹¹S. Colis, G. Gieres, L. Bar, and J. Wecker, *Appl. Phys. Lett.* **83**, 948 (2003).

¹²X. F. Han, S. F. Zhao, F. F. Li, T. Daibou, H. Kubota, Y. Ando, and T. Miyazaki, *J. Magn. Magn. Mater.* **282**, 225 (2004).

¹³X. F. Han, F. F. Li, W. N. Wang, S. F. Zhao, Z. L. Peng, Y. D. Yao, W. S. Zhan, and B. S. Han, *IEEE Trans. Magn.* **39**, 2794 (2003).

¹⁴G. Malinowski, M. Hehn, S. Robert, O. Lenoble, A. Schuhl, and P. Panissod, *Phys. Rev. B* **68**, 184404 (2003).

¹⁵K. Hoshino, R. Nakatani, H. Hoshiya, Y. Sugita, and S. Tunahima, *Jpn. J. Appl. Phys., Part 1* **35**, 607 (1996).

¹⁶K. Nakajima, Y. Saito, S. Nakamura, and K. Inomata, *IEEE Trans. Magn.* **36**, 2806 (2000).

¹⁷J. Barnas and A. Fert, *Phys. Rev. Lett.* **80**, 1058 (1998).

¹⁸A. Brataas, Y. V. Nazarov, J. Inoue, and G. E. W. Bauer, *Phys. Rev. B* **59**, 93 (1999).

¹⁹S. Yuasa, T. Nagahama, and Y. Suzuki, *Science* **297**, 234 (2002).

²⁰T. Valet and A. Fert, *Phys. Rev. B* **48**, 7099 (1993).

²¹S. Zhang, P. M. Levy, A. C. Marley, and S. S. P. Parkin, *Phys. Rev. Lett.* **79**, 3744 (1997).

²²L. Berger, *Phys. Rev. B* **54**, 9353 (1996).